

# Crystal Structure of a Metastable Form of Indium Orthovanadate, InVO<sub>4</sub>-I

M. Touboul<sup>1</sup> and K. Melghit

Laboratoire de Réactivité et de Chimie des Solides, URA CNRS 1211, Université de Picardie Jules Verne, 33 rue Saint-Leu, 80039 Amiens Cedex, France

and

P. Bénard and D. Louër

Laboratoire de Chimie du Solide et Inorganique Moléculaire, URA CNRS 1495, Université de Rennes I, Avenue du Général Leclerc, 35042 Rennes Cedex, France

Received September 12, 1994; in revised form January 18, 1995; accepted January 19, 1995

The compound InVO<sub>4</sub>-I has been obtained with a good purity level from a *chimie douce* process. Using X-ray powder diffraction data, its crystal structure has been determined by analogy with isostructural compounds crystallizing with the so-called  $\alpha$ -MnMoO<sub>4</sub> type structure. The crystal symmetry is monoclinic (space group *C2/m*) and the unit cell parameters are  $a = 10.271(1)$  Å,  $b = 9.403(1)$  Å,  $c = 7.038(1)$  Å, and  $\beta = 105.08(1)^\circ$ . The structure has been refined by the Rietveld method ( $R_F = 0.030$  and  $R_{wp} = 0.098$  for 360 reflections). The structure is based on compact In<sub>4</sub>O<sub>16</sub> groups of four edge-sharing InO<sub>6</sub> octahedra linked to each other by VO<sub>4</sub> tetrahedra. Each In<sub>4</sub>O<sub>16</sub> cluster contains two In1O<sub>6</sub> and two other In2O<sub>6</sub> octahedra and the corresponding In1-O and In2-O mean distances are 2.14 and 2.17 Å. The mean value for the V-O bond length is 1.71 Å. Relationships with the stable indium vanadate and related phases are discussed. © 1995 Academic Press, Inc.

and indium nitrate or, alternatively, from solutions of ammonium vanadate and indium nitrate (2, 4) or indium chloride (5). From infrared spectroscopy, Roncaglia *et al.* (5) found an analogy between InVO<sub>4</sub>-I and compounds crystallizing with the so-called  $\alpha$ -MnMoO<sub>4</sub> type structure (6, 7). The quality of the reported powder diffraction data (4, 5) was generally moderate and additional diffraction lines due to impurities, e.g., In<sub>2</sub>O<sub>3</sub> (5), were often detected. Nevertheless, by using the new method of synthesis described by Touboul *et al.* (3), a pure sample of the metastable phase InVO<sub>4</sub>-I with a better crystallization was obtained. As a consequence, the crystal structure of this phase was investigated from powder diffraction. This study deals with the crystal structure determination of InVO<sub>4</sub>-I from powder diffraction data, collected with monochromatic X rays, and the structural relationships with related phases.

## INTRODUCTION

Among the known varieties of indium vanadate only the crystal structure of the stable form, InVO<sub>4</sub>-III, was established from single-crystal diffraction data (1). In order to compare it with the structure of the metastable form, InVO<sub>4</sub>-I (2), several attempts were made to obtain a pure and well-crystallized phase. In a recent study (3), we reported the synthesis of some indium vanadates, including the preparation of InVO<sub>4</sub>-I by the heating of an amorphous precursor. This precursor was synthesized by *chimie douce* from solutions of xerogel (V<sub>2</sub>O<sub>5</sub> · 1.6H<sub>2</sub>O)

## EXPERIMENTAL

### Synthesis

The amorphous phase, precursor of InVO<sub>4</sub>-I, was synthesized by mixing a solution of indium nitrate, In(NO<sub>3</sub>)<sub>3</sub> · 4.5H<sub>2</sub>O, with a boiling solution of xerogel V<sub>2</sub>O<sub>5</sub> · 1.6H<sub>2</sub>O. The xerogel was obtained after drying, at room temperature, the gel formed from a solution of vanadic acid. This solution was prepared by acidification of a sodium vanadate (NaVO<sub>3</sub>) solution obtained by passing it through a cation (H<sup>+</sup>) exchange resin. After stirring the boiling mixture for a few minutes a precipitate with the formula InVO<sub>4</sub> · 2.4 H<sub>2</sub>O was obtained. After annealing at 400°C for 6 hr a crystalline phase of InVO<sub>4</sub>-I was obtained.

<sup>1</sup> To whom correspondence should be addressed.

### X-Ray Diffraction Data Collection

X-ray powder diffraction data were collected at 23°C with a Siemens D500 powder diffractometer, using the Bragg–Brentano geometry. Monochromatic  $\text{CuK}\alpha_1$  X rays were obtained using an incident-beam germanium monochromator with asymmetric focusing (short focal distance, 124 mm; long focal distance, 216 mm). The specimen surface area was completely illuminated at about  $12^\circ$  ( $2\theta$ ). The alignment of the diffractometer was checked by means of standard reference materials and the accuracy at low angles was evaluated using 00 $l$  reflections of fluorophlogopite mica reference material from NIST (SRM 675). The zero error was measured as less than  $0.01^\circ$  ( $2\theta$ ). The instrumental resolution function (IRF) for this conventional powder diffractometer, obtained from an annealed barium fluoride sample, shows a shallow minimum at about  $40^\circ$  ( $2\theta$ ), with a FWHM value of  $0.065^\circ$  ( $2\theta$ ) (8). The powder diffraction pattern was scanned in steps of  $0.02^\circ$  ( $2\theta$ ) over the angular range from 9 to  $100^\circ$  ( $2\theta$ ) and a fixed counting time (12 sec) was employed. After data collection, the stability of the incident X-ray beam was checked by recording the first lines of the pattern. No significant preferred orientation effects were detected. From the fitting by pseudo-Voigt functions of some individual diffraction lines, in the low angle range 12– $40^\circ$  ( $2\theta$ ), the average FWHM value  $0.25^\circ$  ( $2\theta$ ) was obtained. With regard to the IRF, it is an indication that the sample exhibits important diffraction line broadening due to intrinsic size and/or microstrain effects. However, the quality of the pattern was not good enough for a detailed analysis of these crystal imperfections.

### Structure Determination

The indexing of the powder diffraction pattern of  $\text{InVO}_4\text{-I}$  was reported recently (3). The unit cell was found to be monoclinic with the figures of merit  $M_{20} = 21$  and  $F_{30} = 46(0.009, 75)$ . From this solution apparent isostructural relationships have been detected with  $\alpha\text{-MnMoO}_4$  (6) ( $a = 10.469 \text{ \AA}$ ,  $b = 9.516 \text{ \AA}$ ,  $c = 7.143 \text{ \AA}$ ,  $\beta = 106.3^\circ$ , and space group  $C2/m$ ),  $\beta\text{-CdCrO}_4$ , and  $\beta\text{-MgCrO}_4$  (7). After refinement of the unit cell parameters by the program NBS\*AIDS83 (9), from the powder diffraction data available in the pattern, the cell parameters of  $\text{InVO}_4\text{-I}$  are  $a = 10.271(1) \text{ \AA}$ ,  $b = 9.403(1) \text{ \AA}$ ,  $c = 7.038(1) \text{ \AA}$ ,  $\beta = 105.08(1)^\circ$ , and  $V = 656.3(1) \text{ \AA}^3$  and the corresponding figures of merit, taking into account the absences due to the space group  $C2/m$ , are  $M_{20} = 41$  and  $F_{30} = 73(0.0096, 43)$ . The observed density,  $4.650 \text{ g} \cdot \text{cm}^{-3}$ , is in agreement with the calculated value,  $4.672 \text{ g} \cdot \text{cm}^{-3}$ , for  $Z = 8$ . The atomic coordinates of  $\alpha\text{-MnMoO}_4$  (6) were used as starting parameters for the structure refinement of  $\text{InVO}_4\text{-I}$ , assuming the space group  $C2/m$ . They were input in the program FULLPROF (10), derived from the Rietveld pro-

TABLE 1  
Details of Rietveld Refinement for  $\text{InVO}_4\text{-I}$

Space group	$C2/m$
$Z$	8
Wavelength ( $\text{\AA}$ )	1.540598
Step scan increment ( $^\circ$ ) ( $2\theta$ )	0.02
$2\theta$ Range ( $^\circ$ )	9–100
No. of reflections	360
No. of profile parameters	14
No. of structural parameters	25
No. of atoms	9
$R_F$	0.030
$R_B$	0.037
$R_p$	0.074
$R_{wp}$	0.098

Note. The  $R$  factors are defined as

$$R_F = \frac{\sum |I(\text{obs})^{1/2} - I(\text{calc})^{1/2}|}{\sum I(\text{obs})^{1/2}}$$

$$R_B = \frac{\sum |I(\text{obs}) - I(\text{calc})|}{\sum I(\text{obs})}$$

$$R_p = \frac{\sum |y_i(\text{obs}) - (1/c)y_i(\text{calc})|}{\sum y_i(\text{obs})}$$

$$R_{wp} = \left[ \frac{\sum \omega_i [y_i(\text{obs}) - (1/c)y_i(\text{calc})]^2}{\sum \omega_i [y_i(\text{obs})]^2} \right]^{1/2}$$

gram DBW3.2S(8804) (11), running on a PC computer. The final refinement, carried out in the range 9– $100^\circ$  ( $2\theta$ ), involved the following parameters: one scale factor, 24 structural parameters including five isotropic temperature factors (the temperature factors of the oxygen atoms were allowed to vary in the same manner), one mixing parameter to define a  $\theta$ -dependent pseudo-Voigt profile shape, three half-width parameters ( $U$ ,  $V$ ,  $W$ ) to describe the angular dependence of the peak FWHM using the usual quadratic form in  $\tan \theta$ , one zero-point, four unit-cell dimensions, and five coefficients in a polynomial function describing the background. The details of the refinement are given in Table 1. Figure 1 displays the final Rietveld plot showing the good agreement between observed and calculated patterns. This fit corresponds to satisfactory profile factors ( $R_p = 0.074$ ,  $R_{wp} = 0.098$ ) and structure model indicators ( $R_B = 0.037$ ,  $R_F = 0.030$ ). This result confirms the isostructural relationships with  $\alpha\text{-MnMoO}_4$ ,  $\beta\text{-CdCrO}_4$ , and  $\beta\text{-MgCrO}_4$ . The final atomic parameters are given in Table 2 and selected bond distances and angles are given in Table 3.

### RESULTS AND DISCUSSION

The structure of the metastable form  $\text{InVO}_4\text{-I}$  can be described from that of  $\alpha\text{-MnMoO}_4$  by replacing the two

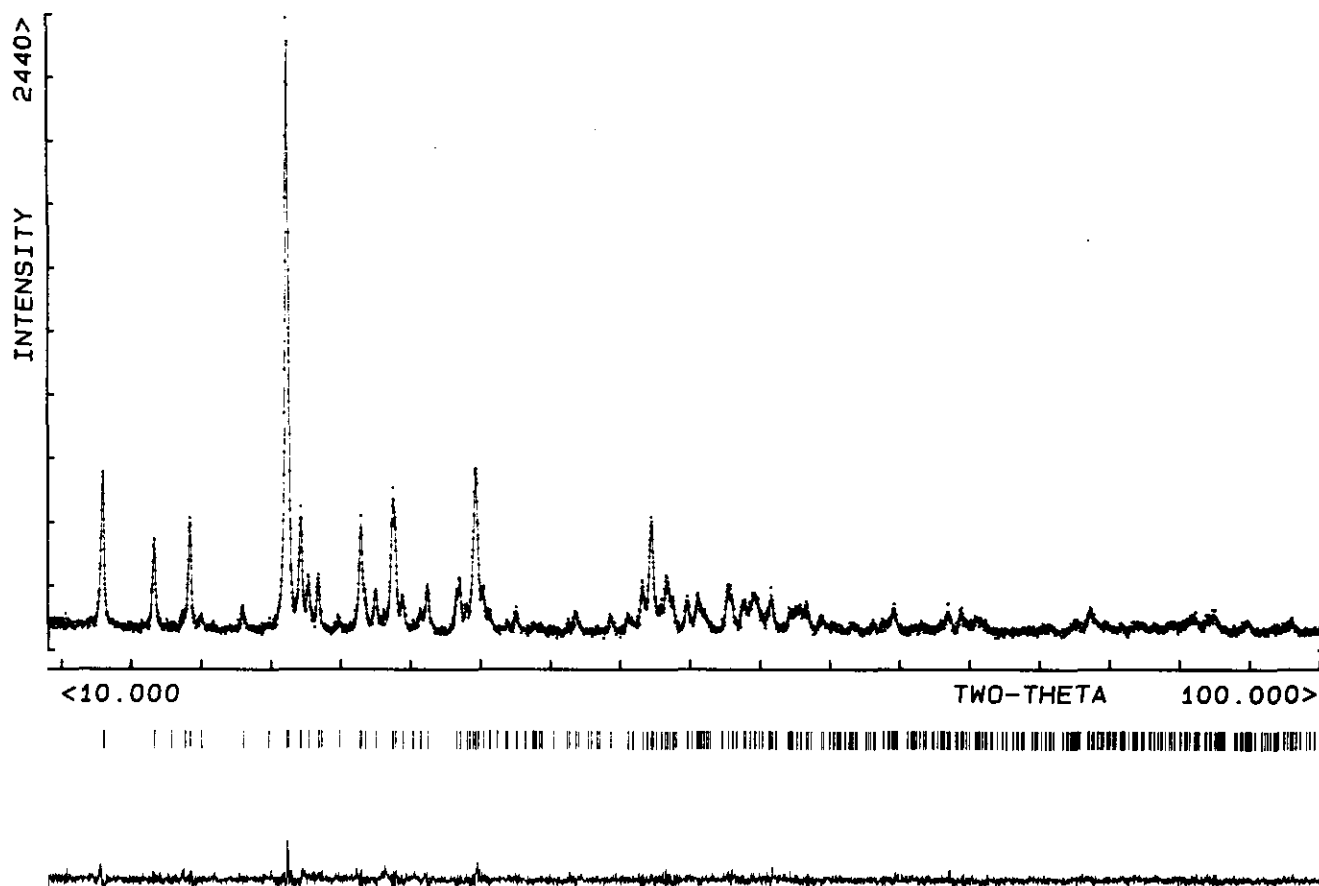


FIG. 1. Final Rietveld plot for  $\text{InVO}_4\text{-I}$ . The upper trace shows the observed data as dots and the calculated pattern is shown by the solid line. The lower trace is a plot of the difference: observed minus calculated. The vertical markers show the positions calculated for Bragg reflections.

crystallographically independent Mn atoms by two In atoms, In1 and In2, and the two Mo atoms by two V atoms, V1 and V2. The two In atoms are octahedrally coordinated by oxygen atoms and the V atoms are surrounded by distorted oxygen tetrahedra (see Table 3). It

TABLE 2  
Atomic Coordinates and Isotropic Thermal Parameters ( $\text{\AA}^2$ )  
with Their Standard Deviations for  $\text{InVO}_4\text{-I}$

Atom	x	y	z	$B_{\text{iso}}$
In1	0.0	0.1875(3)	0.5	0.3(1)
In2	0.7907(3)	0.0	0.1313(5)	0.9(1)
V1	0.0	0.2563(7)	0.0	0.7(2)
V2	0.2737(9)	0.0	0.402(1)	0.3(2)
O1	0.141(2)	0.5	0.541(4)	0.2(2)
O2	0.789(2)	0.0	-0.169(4)	0.2(2)
O3	0.636(2)	0.153(1)	0.107(2)	0.2(2)
O4	0.044(2)	0.161(2)	0.808(3)	0.2(2)
O5	0.136(2)	0.350(2)	0.522(2)	0.2(2)

can be noted that the structure of the stable orthorhombic phase  $\text{InVO}_4\text{-III}$  is also characterized by the two basic  $\text{InO}_6$  and  $\text{VO}_4$  units (1). Figure 2a represents a partial projection of the structure on the  $ab$  plane, in which  $\text{VO}_4$  groups are omitted for clarity and Fig. 2b is the projection of these  $\text{VO}_4$  tetrahedra on the same plane. The (001) octahedral projection shows that the structure of  $\text{InVO}_4\text{-I}$  consists of  $\text{In}_4\text{O}_{16}$  clusters of four edge-sharing  $\text{InO}_6$  polyhedra linked to similar units, in the direction of the  $c$ -axis, through the  $\text{VO}_4$  groups shown in Fig. 2b.

Each  $\text{In}_4\text{O}_{16}$  group is formed by one pair of  $\text{InO}_6$  octahedra joined by a common edge O1-O1 running along the [010] direction, with In1 atoms at  $z_{\text{In1}} = 0.50$ , and two  $\text{In}_2\text{O}_6$  polyhedra on both sides of the pair, located at  $z_{\text{In2}} = 0.13$  and  $z_{\text{In2}} = 0.87$  (see Fig. 2a). Each  $\text{In}_2\text{O}_6$  polyhedron shares their two O1-O4 edges with one pair of  $\text{InO}_6$ . Similar descriptions were recently reported for  $\alpha\text{-Mn-MoO}_4$  (12) and the solid solutions  $\text{Cr}_x\text{Fe}_{1-x}\text{VO}_4\text{-I}$  (13, 14) in order to explain the magnetic behavior in these materials. The five independent oxygen atoms in  $\text{InVO}_4\text{-I}$  may be divided into three groups according to their coordination

mode in the structure: O2, O3, and O5 atoms common to one octahedron and one tetrahedron, O4 shared by two different octahedra (In1O<sub>6</sub> and In2O<sub>6</sub>) and one tetrahedron, and O1 common to three octahedra (two In1O<sub>6</sub> and one In2O<sub>6</sub>) and one tetrahedron V2O<sub>4</sub> (Fig. 3). This feature is consistent with the distribution of the In–O distances in which the five In–O mean values range according to the sequence In–O5 (2.05 Å) < In–O2 (2.11 Å) < In–O3 (2.12 Å) < In–O4 (2.17 Å) < In–O1 (2.24 Å). The In<sub>4</sub>O<sub>16</sub> entities do not exist in the structure of the orthorhombic stable phase InVO<sub>4</sub>-III (1), which is built from chains of equivalent InO<sub>6</sub> octahedra linked together by VO<sub>4</sub> tetrahe-

TABLE 3  
Selected Interatomic Distances (Å) and Angles (°) with Their Standard Deviations for InVO<sub>4</sub>-I

Within the InO <sub>6</sub> octahedra							
In1	-O1	2.25(1)	In2	-O1 <sup>II</sup>	2.23(3)		
	-O1 <sup>I</sup>		In2	-O2	2.11(3)		
In1	-O4	2.11(2)	In2	-O3	2.12(3)		
	-O4 <sup>I</sup>		In2	-O3 <sup>III</sup>			
In1	-O5	2.05(2)	In2	-O4 <sup>II</sup>	2.23(2)		
	-O5 <sup>I</sup>		In2	-O4 <sup>IV</sup>			
Mean In1–O distance = 2.14			Mean In2–O distance = 2.17				
O1–	In1	-O1 <sup>I</sup>	77(1)	O1 <sup>II</sup> –	In2	-O2	163(10)
		-O4	79(1)			-O3	96(1)
		-O4 <sup>I</sup>	90(1)			-O3 <sup>III</sup>	96(1)
O1 <sup>I</sup> –	In1	-O4	90(1)			-O4 <sup>II</sup>	77(1)
		-O4 <sup>I</sup>	79(1)			-O4 <sup>IV</sup>	77(1)
O1–	In1	-O5	100(1)	O2–	In2	-O3	96(2)
		-O5 <sup>I</sup>	175(10)			-O3 <sup>III</sup>	96(2)
O1 <sup>I</sup> –	In1	-O5	175(1)			-O4 <sup>II</sup>	90(1)
		-O5 <sup>I</sup>	100(1)			-O4 <sup>IV</sup>	90(1)
O4–	In1	-O4 <sup>I</sup>	166(9)	O3–	In2	-O3 <sup>III</sup>	85(1)
		-O5	93(1)			-O4 <sup>II</sup>	94(1)
		-O5 <sup>I</sup>	97(1)			-O4 <sup>IV</sup>	174(10)
O4 <sup>I</sup> –	In1	-O5	97(1)	O3 <sup>III</sup> –	In2	-O4 <sup>II</sup>	174(10)
		-O5 <sup>I</sup>	93(1)			-O4 <sup>IV</sup>	94(1)
O5–	In1	-O5 <sup>I</sup>	84(1)	O4 <sup>II</sup> –	In2	-O4 <sup>IV</sup>	86(1)
Within the VO <sub>4</sub> tetrahedra							
V1	-O3 <sup>V</sup>	1.64(2)	V2	-O1	1.87(3)		
	-O3 <sup>VI</sup>		V2	-O2 <sup>VIII</sup>	1.59(3)		
V1	-O4 <sup>I</sup>	1.78(2)	V2	-O5 <sup>IX</sup>	1.69(2)		
	-O4 <sup>VII</sup>		V2	-O5 <sup>X</sup>			
Mean V1–O distance = 1.71			Mean V2–O distance = 1.71				
O3 <sup>V</sup> –	V1	-O3 <sup>VI</sup>	117(2)	O1–	V2	-O2 <sup>VIII</sup>	113(3)
		-O4 <sup>I</sup>	105(2)			-O5 <sup>IX</sup>	104(2)
		-O4 <sup>VII</sup>				-O5 <sup>X</sup>	
O3 <sup>VI</sup> –	V1	-O4 <sup>I</sup>	106(2)	O2–	V2	-O5 <sup>IX</sup>	111(2)
		-O4 <sup>VII</sup>				-O5 <sup>X</sup>	
O4 <sup>I</sup> –	V1	-O4 <sup>VII</sup>	119(2)	O5 <sup>IX</sup> –	V2	-O5 <sup>X</sup>	113(2)

Note. Symmetry code: I,  $-x, y, 1-z$ ; II,  $1-x, y, 1-z$ ; III,  $x, -y, z$ ; IV,  $1-x, -y, 1-z$ ; V,  $x - \frac{1}{2}, \frac{1}{2} - y, z$ ; VI,  $\frac{1}{2} - x, \frac{1}{2} - y, -z$ ; VII,  $x, y, z - 1$ ; VIII,  $1 - x, y, -z$ ; IX,  $\frac{1}{2} - x, \frac{1}{2} - y, 1 - z$ ; X,  $x - \frac{1}{2}, y - \frac{1}{2}, 1 - z$ .

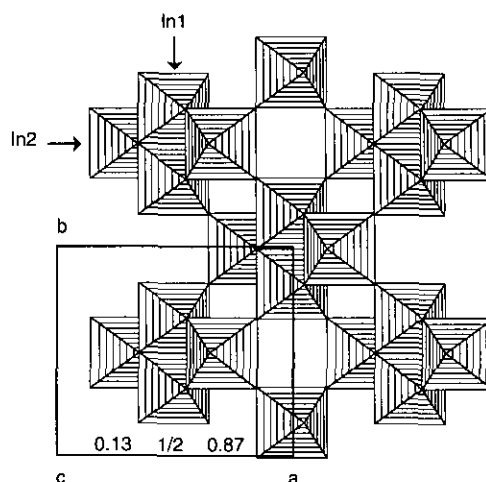


FIG. 2a. Partial projection of the structure of InVO<sub>4</sub>-I on the *ab* plane showing only InO<sub>6</sub> octahedra in terms of In<sub>4</sub>O<sub>16</sub> clusters; the *z* coordinates of indium atoms of one In<sub>4</sub>O<sub>16</sub> group are indicated.

dra. The In–O distances spread in the range 2.160(3) to 2.162(3) Å, showing that distortions within the polyhedra InO<sub>6</sub> may be considered negligible within one standard deviation. In the structure of the metastable phase InVO<sub>4</sub>-I, there is a significant variation in the In–O distances (from 2.05 to 2.25 Å), particularly within the In1 coordination sphere which exhibits two short bond lengths (2.05 Å), two medium bond lengths (2.11 Å), and two longer bond lengths (2.25 Å). Although it is known that the accuracy of the atomic positions derived from powder diffraction data cannot rival the precision reached from single-crystal data, it is interesting to note that similar Mn1–O bond lengths were found for  $\alpha$ -MnMoO<sub>4</sub> (2.098, 2.148, and 2.252 Å) (6). The sixfold coordination sphere is slightly less distorted for In2, with three bond lengths close to 2.12 Å and three others equal to 2.23 Å,

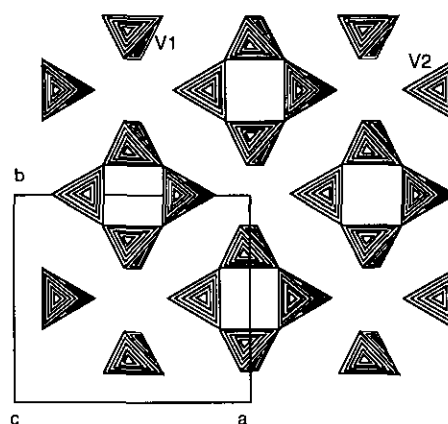


FIG. 2b. Partial projection of the structure of InVO<sub>4</sub>-I on the *ab* plane showing only vanadate tetrahedra.

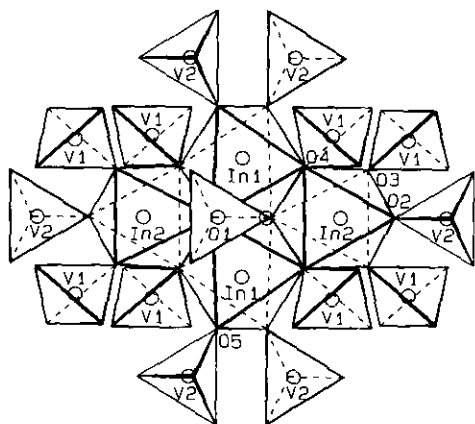


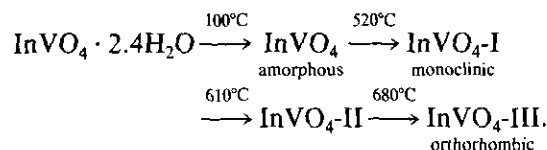
FIG. 3. Structure of  $\text{InVO}_4\text{-I}$  in the (102) plane showing one  $\text{In}_4\text{O}_{16}$  group sharing all its corners with 16 independent  $\text{VO}_4$  tetrahedra. The positions of indium and vanadium atoms are indicated by small circles.

whereas for  $\alpha\text{-MnMoO}_4$  the  $\text{Mn2-O}$  distances are in the range 2.091–2.227 Å (6). The corresponding mean value, 2.164(7) Å, compares well with that obtained for  $\text{InVO}_4\text{-I}$ , i.e., 2.16(2) Å. This last value is in accordance, within one standard deviation, with the mean value (2.18 Å) commonly found in  $\text{InO}_6$  octahedra (see Ref. 1). The deviation of the octahedra from  $O_h$  symmetry, though smaller, is also observed in the solid solutions  $\text{Cr}_x\text{Fe}_{1-x}\text{VO}_4\text{-I}$  ( $x = 0.20, 0.25, 0.50, 0.75,$  and  $0.80$ ) (13, 14).

There are two independent  $\text{VO}_4$  tetrahedra in the asymmetric unit cell of  $\text{InVO}_4\text{-I}$ . Both  $\text{V1O}_4$  and  $\text{V2O}_4$  groups play a major role in bridging the  $\text{In}_4\text{O}_{16}$  clusters between them. As displayed in Fig. 3 they are involved in the 16 corners of each  $\text{In}_4\text{O}_{16}$  unit and each tetrahedron shares four different  $\text{In}_4\text{O}_{16}$  clusters. The  $\text{V2O}_4$  group differs from  $\text{V1O}_4$  by one oxygen common to three octahedra from the same  $\text{In}_4\text{O}_{16}$  unit. The maximum deviations of  $\text{V-O}$  lengths from the mean value (1.71 Å) are 0.07 and 0.16 Å for  $\text{V1-O}$  and  $\text{V2-O}$ , respectively. The individual  $\text{O-V-O}$  angles vary from 104 to 119°, with mean values (109.66° for  $\text{O-V1-O}$  and 109.33° for  $\text{O-V2-O}$ ) close to the ideal tetrahedral angle. It can be noted that  $\text{V2O}_4$  is more distorted ( $\text{V2-O}$  distances in the range 1.59–1.87 Å) than  $\text{V1O}_4$  ( $\text{V1-O}$  distances: 1.64 and 1.78 Å). These results compare well with the values observed in  $\text{InVO}_4\text{-III}$  (1.662 and 1.791 Å). Moreover, the two identical mean  $\text{V-O}$  distances (1.71 Å) agree well with those reported for  $\text{Cr}_x\text{Fe}_{1-x}\text{VO}_4\text{-I}$  (1.723 Å for  $x = 0.2$ ) (13).

The results of the bond–valence calculations (15) from the  $\text{InVO}_4\text{-III}$  and  $\text{InVO}_4\text{-I}$  structures are given in Table 4. For  $\text{InVO}_4\text{-III}$  the bond–valence rule is fully respected while the agreement is not as good for  $\text{InVO}_4\text{-I}$ , particularly for O2, In1, and V atoms. This deviation can be expected in crystal structures derived from powder diffraction.

As indicated before, some divalent metal molybdates and chromates have a structure similar to that of  $\text{InVO}_4\text{-I}$ :  $\beta\text{-MgCrO}_4$  and  $\beta\text{-CdCrO}_4$ , which were found in the study of the  $\text{MO-Cr}_2\text{O}_3\text{-O}$  systems ( $M = \text{Mg, Cd}$ ) at high oxygen pressure (7, 16);  $\alpha\text{-MnMoO}_4$ ,  $\text{MgMoO}_4$ ,  $\text{FeMoO}_4$ ,  $\text{CoMoO}_4$ , and  $\text{NiMoO}_4$  (6, 17–21), which were generally synthesized by the classical ceramic route from a mixture of oxides. Some of these compounds also crystallize with another structure: wolframite type (monoclinic) for  $\text{MgMoO}_4$ ,  $\text{MnMoO}_4$ ,  $\text{CoMoO}_4$  (22); scheelite type (tetragonal) for  $\text{CdCrO}_4$  (23) synthesized under very high pressure (40–60 kbars); and  $\text{InVO}_4\text{-III}$  type for some chromates such as  $\alpha\text{-CdCrO}_4$ ,  $\alpha\text{-MgCrO}_4$ , and  $\text{NiCrO}_4$  (7). Finally, it is interesting to compare the conditions of synthesis for the different forms of  $\text{MCrO}_4$  ( $M = \text{Mg, Cd}$ ) and  $\text{InVO}_4$ . The phases  $\alpha\text{-MCrO}_4$ , with the  $\text{InVO}_4\text{-III}$  type structure, were obtained under 1 kbar oxygen pressure at 500–600°C, while the phases  $\beta\text{-MCrO}_4$  ( $\text{InVO}_4\text{-I}$  type structure) were obtained under the same pressure but at higher temperature (700–800°C) (7). Moreover, different forms of  $\text{InVO}_4$  can be obtained by heating the amorphous phase  $\text{InVO}_4 \cdot 2.4\text{H}_2\text{O}$  according to the transformation scheme (3):



However, the phase  $\text{InVO}_4\text{-II}$  has not been characterized because it exists in a narrow temperature range. There is

TABLE 4  
Bond–Valence Calculations for  $\text{InVO}_4\text{-III}$  (a) and  $\text{InVO}_4\text{-I}$  (b)

	(a)					$\Sigma_{\text{exp}}$	$\Sigma_{\text{th}}$
	O1	O2					
In	$0.50 \times 4$	$0.50 \times 2$				3	3
V	$1.03 \times 2$	$1.46 \times 2$				4.98	5
$\Sigma_{\text{exp}}$	2.03	1.96					
$\Sigma_{\text{th}}$	2	2					
	(b)					$\Sigma_{\text{exp}}$	$\Sigma_{\text{th}}$
	O1	O2	O3	O4	O5		
In1	$0.39 \times 2$			$0.57 \times 2$	$0.67 \times 2$	3.26	3
In2	0.41	0.57	$0.55 \times 2$	$0.41 \times 2$		2.9	3
V1			$1.55 \times 2$	$1.06 \times 2$		5.22	5
V2	0.83	1.78			$1.36 \times 2$	5.33	5
$\Sigma_{\text{exp}}$	2.02	2.35	2.1	2.04	2.03		
$\Sigma_{\text{th}}$	2	2	2	2	2		

Note.  $s = \exp [r_0 - r]/B$  with  $B = 0.37$  and  $r_0 = 1.902$  Å for  $\text{In}^{3+}$ ,  $r_0 = 1.803$  Å for  $\text{V}^{5+}$  (from Ref. 15). For  $\text{InVO}_4\text{-III}$ , all data were taken from Ref. (1).

no comparable study of the transformations in the divalent metal chromates and molybdates, even though  $\text{CdCrO}_4$  exists under three forms. It is also interesting to note that the solid solutions  $\text{Cr}_x\text{Fe}_{1-x}\text{VO}_4$ -I, which have the  $\alpha$ - $\text{MnMoO}_4$  (and  $\text{InVO}_4$ -I) type structure at atmosphere pressure, exhibit a reversible transformation, at 3000 atm pressure, into an  $\text{InVO}_4$ -III type structure (13). A behavior analogous to that of  $\text{InVO}_4$  was recently reported for  $\text{CrVO}_4$  (24). A new form,  $\text{CrVO}_4$ -I, with the  $\alpha$ - $\text{MnMoO}_4$  type structure was synthesized by *chimie douce*, leading by heating to the stable form,  $\text{CrVO}_4$ -III, with the same structure as  $\text{InVO}_4$ -III (25). All these results show that several structural types may be encountered in the  $\text{ABO}_4$  compounds (wolframite, scheelite,  $\text{InVO}_4$ -I, and  $\text{InVO}_4$ -III structural types), but the preparative conditions to predict the structure of a phase are not still clear.

To conclude, although the X-ray powder diffraction pattern of the metastable phase of indium vanadate exhibits significant diffraction line broadening, its crystal structure has been determined with enough precision for a discussion of the structural features. The result sheds new light on the complex chemistry of indium vanadates.

## REFERENCES

1. M. Touboul and P. Tolédano, *Acta Crystallogr. Sect. B* **36**, 240 (1980).
2. M. Touboul and D. Ingrain, *J. Less-Common Met.* **71**, 55 (1980).
3. M. Touboul, K. Melghit, and P. Bénard, *Eur. J. Solid State Inorg. Chem.* **31**, 151, (1994).
4. M. Touboul and A. Popot, *Rev. Chim. Miner.* **22**, 610 (1985).
5. D. I. Roncaglia, I. L. Botto, and E. J. Baran, *J. Solid State Chem.* **62**, 11 (1986).
6. S. C. Abrahams and J. M. Reddy, *J. Chem. Phys.* **43**, 2533 (1965).
7. O. Müller, W. B. White, and D. Roy, *Z. Kristallogr.* **130**, 112 (1969).
8. D. Louër and J. I. Langford, *J. Appl. Crystallogr.* **21**, 430 (1988).
9. A. D. Mighell, C. R. Hubbard, and J. K. Stalick, "NBS\* AIDS83: an Expanded Version of NBS\* AIDS80, a Fortran Program for Crystallographic Data Evaluation." Technical Note 1141. Nat. Bur. Stand. (now National Institute of Standards and Technology), Gaithersburg, MD, 1981.
10. J. Rodriguez-Carvajal, in "Collected Abstracts of Powder Diffraction Meeting, Toulouse, France, July 1990," p. 127.
11. D. B. Wiles, A. Sakthivel, and R. A. Young, in "User's Guide to Program DBW3.2S (Version 8804)," Georgia Institute of Technology, Atlanta, 1988.
12. J. P. Attfield, *J. Phys. Condens. Matter* **2**, 6999 (1990).
13. J. P. Attfield, *J. Solid State Chem.* **67**, 58 (1987).
14. J. P. Attfield, A. K. Cheetham, D. C. Johnson, and T. Novet, *J. Mater. Chem.* **1**, 867 (1991).
15. I. D. Brown and D. Altermatt, *Acta Crystallogr. Sect. B* **41**, 244 (1985).
16. O. Müller, R. Roy, and W. B. White, *J. Am. Ceram. Soc.* **51**, 693 (1968).
17. National Bureau of Standards Monograph 25, Section 7. p. 28, Natl. Bur. Stand., Washington, DC, 1969.
18. A. W. Sleight and B. L. Chamberland, *Inorg. Chem.* **7**, 1672 (1968).
19. G. W. Smith, *Acta Crystallogr.* **19**, 269 (1965).
20. L. M. Plyasova, V. I. Zharkov, G. N. Kustova, L. G. Karakchiev, and M. M. Andruskevich, *Izv. Akad. Nauk SSSR Neorg. Mater.* **9**, 519 (1973).
21. National Bureau of Standards Monograph 24, Section 19. p. 62, Natl. Bur. Stand., Washington, DC, 1982.
22. A. P. Young and C. M. Schwartz, *Science* **141**, 348 (1963).
23. O. Müller, F. Dacheille, W. B. White, and D. Roy, *Inorg. Chem.* **9**, 410 (1970).
24. (a) M. Touboul and K. Melghit, Soft Chemistry Routes to New Materials: An International Symposium, Nantes, France, 1993; (b) K. Melghit, Thesis, Université de Picardie Jules Verne, Amiens, 1994; (c) M. Touboul and K. Melghit, *J. Mater. Chem.* **5**, 147 (1995).
25. M. J. Isasi, R. Saez-Püche, M. L. Veiga, C. Pico, and A. Jerez, *Mater. Res. Bull.* **23**, 595 (1988).